Available online at www.sciencedirect.com
SCIENCE DIRECT®
Journal of Nuclear Materials 341 (2005) 153–163
journal of nuclear materials
www.elsevier.com/locate/jnucmat

Positron annihilation study of effects of Ti and plastic deformation on defect accumulation and annealing in electron-irradiated austenitic steels and alloys

A.P. Druzhkov *, V.L. Arbuzov, D.A. Perminov

Institute of Metal Physics, Ural Branch RAS, 18 Kovalevskaya St., 620219 Ekaterinburg GSP-170, Russia

Received 25 May 2004; accepted 19 January 2005

Abstract

Positron annihilation spectroscopy was used to study the formation and annealing of vacancy clusters in 16Cr15Ni3Mo austenitic steels and Fe–36%Ni model alloys and in the same compounds containing 1.02 and 2.5 wt% titanium respectively. Defects were induced by electron (5 MeV) irradiation at 270–573 K. How a developed initial dislocation structure influenced the accumulation and annealing of vacancy defects in these steels and alloys was analyzed. It was shown that vacancies interacted with titanium atoms. As a result, the Ti-containing steels and alloys exposed to radiation at temperatures from 270 to 423 K had an enhanced concentration of fine vacancy clusters decorated with titanium, which were thermally stable up to 450 K. A high initial dislocation density in the deformed steels and alloys led to a several-fold decrease in the concentration of vacancy clusters as compared to their concentration in the solution annealed state. The formation of fine TiC particles in Ti-modified deformed steel was monitored at the annealing temperatures from 850 to 1070 K.

PACS: 61.72.Ji; 61.72.Lk; 61.82.Bg; 78.70.Bj

1. Introduction

Austenitic stainless steels have been adopted as materials for fast breeder reactor core applications. Many efforts at improving their strength at elevated temperature and void swelling resistance have been made to prolong their lives. It was found that over-sized impurities (for example, Nb and Ti) influence the vacancy mobility in austenitic steels and alloys [1]. Moreover, addition of more than 0.3 wt% titanium in combination with thermomechanical treatment facilitates the formation of fine TiC precipitates, which decrease void swelling [2,3] and helium embrittlement [4]. It was shown [5] that high-temperature irradiation of a Ti-modified stainless steel caused appearance of γ'-phase particles, which also impede void swelling.

Preliminary cold deformation also retards void swelling of stainless steels [6]. However, a locally inhomogeneous microstructure is formed in austenitic alloys and steels during deformation. Processes of the radiation

* Corresponding author. Tel.: +7 343 378 38 62; fax: +7 343 374 52 44.
E-mail address: druzhkov@imp.uran.ru (A.P. Druzhkov).

0022-3115/$ - see front matter © 2005 Elsevier B.V. All rights reserved.
doi:10.1016/j.jnucmat.2005.01.021

damage in materials having an inhomogeneous distribution of dislocations are not quite clear. Also, a developed dislocation structure of steels has a considerable effect on the phase stability when they are irradiated at high temperatures or undergo thermal treatment. It is well known [7] that dislocations are annealed over one and the same temperature interval, leading to precipitation of carbides and intermetallics.

The present study is concerned with the accumulation and annealing of vacancy-type defects in Fe–Cr–Ni and Fe–Ni solid solutions with and without titanium additions. The effect of a developed dislocation structure of these steels on the evolution of defects was analyzed. Radiation defects were induced by electron radiation, which generated homogeneously distributed Frenkel pairs. Defects were diagnosed using a positron annihilation spectroscopy (PAS) whose physical principles are described comprehensively in [8,9]. PAS is highly sensitive to single vacancies and their aggregates in the form of clusters, loops and nanovoids [10]. It is well known also that positrons are sensitive to dislocations in metals and alloys [11].

However, some authors [12,13] revealed a low sensitivity of positrons to dislocations in austenitic stainless steels. At least they fond no a correlation between annihilation parameter measurements and the dislocation density determined by transmission electron microscopy (TEM) after cold-rolling. In this study we tried to elucidate the situation with the positron trapping by dislocations in austenitic steels.

2. Materials and methods

Samples of the reactor steel type 16Cr15Ni3Mo1Ti (SS-Ti) (containing, wt%, 15.9 Cr, 15.0 Ni, 2.5 Mo, 1.02 Ti, 0.03 C, the balance Fe), Ti-free (<0.02) steel type 16Cr15Ni3Mo (SS) of a similar composition, and Fe–36.5Ni (Fe–Ni) and Fe–36.5Ni–2.5 Ti (Fe–Ni–Ti) fcc alloys (wt%) were used. After rolling, cutting and electrical polishing, the samples were annealed under a 10^{-6} Pa vacuum at 1373 K for 1 h and then were cooled quickly (~500 K/s). The presence of one austenitic phase in the samples was checked by the X-ray analysis.

Some steel and alloy samples were deformed by rolling to 25–40% at room temperature. The microstructure of the solution annealed and deformed samples were certified using a JEM-200 CX electron microscope at the accelerating voltage of 160 kV. The samples of the solution annealed steels and alloys (the SA state) had grains ~30 μm in size and the dislocation density of about 10^{11} m^{-2}. The TEM analysis of the steels in the SA state revealed single coarse particles 100–500 nm in size, which probably had the metallurgical origin. Some coarse particles in the SS-Ti steel samples were identified as TiC carbides, which did not dissolve during thermal treatment similarly to the results obtained in [14].

The samples of dimensions 10 mm × 10 mm × 0.2 mm were irradiated at 270–573 K with 5 MeV electrons in a linear accelerator. The sample was positioned as tightly as possible in the centre of irradiation zone (10 × 10 mm) of sample holder and electron beam sweeping was applied to provide homogeneous irradiation. The temperature control accuracy during irradiation was ±5 K. The maximum electron fluence was 5×10^{22} m^{-2}, which corresponded to the damaging dose of $(2–3) \times 10^{-4}$ dpa as calculated by the modified Kinchin–Pease model [15].

The irradiated samples were annealed stepwise (25–50 K per step) in a vacuum over the temperature interval from 300 to 1300 K at an average heating rate of 1 K min^{-1}.

A one-dimensional angular correlation annihilation radiation (ACAR) spectrometer (one of the PAS methods) with a resolution of 1 mrad × 160 mrad was used [16]. A ^{68}Ge positron source of activity of ~300 MBq was used. At the least 3×10^5 counts were collected in each ACAR spectrum. Changes in the shape of ACAR spectra due to positron trapping by defects were characterized by standard S, W and R-parameters [16].

3. Experimental results

3.1. Accumulation and annealing of defects in alloys and steels (initial SA state)

3.1.1. Model alloys

Fig. 1 presents the dependence of the S-parameter on the electron fluence for Fe–Ni and Fe–Ni–Ti alloys irradiated at 270, 423 and 573 K. In the initial state (before irradiation) the S-parameters of the two alloys had similar values corresponding to annihilation of positrons from free states, because the concentration of quenched vacancies in austenitic alloys usually is lower than the PAS sensitivity limit [13] since thermal conductivity of these alloys is low. The S-parameter increased with the fluence in both samples at all the irradiation temperatures. The growth of the S-parameter was most intensive at 270 K. In [17] we demonstrated that vacancies were mobile in the Fe–Ni alloy already at 270 K and formed three-dimensional vacancy clusters (VCs) during their migration. The capture of positrons by these clusters led to the growth of the S-parameter over S_v for single vacancies [17]. Therefore, the main emphasis will be on the Fe–Ni–Ti alloy. The S-parameter of this titanium-doped alloy increased more intensively than its counterpart in the Fe–Ni alloy at 270 K. At a fluence of 5×10^{22} m^{-2} values of the S-parameter in Fe–Ni–Ti were much larger, i.e. titanium stimulated the growth of the concentration of vacancy clusters.

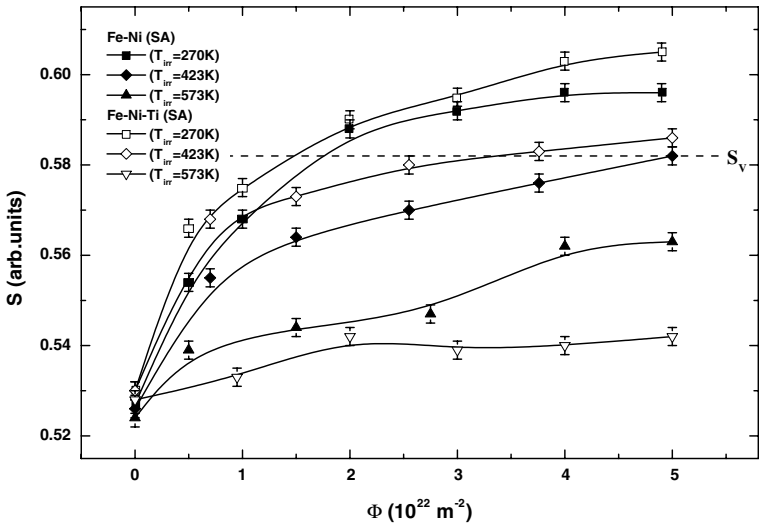

Fig. 1. *S*-parameter variation versus irradiation fluence at 270, 423, 573 K Fe–Ni and Fe–Ni–Ti austenitic alloys, respectively. The initial solution annealed (SA) state of the samples.

An analogous situation was observed at the irradiation temperature of 423 K (Fig. 1). Values of the *S*-parameter in the titanium-doped alloy were larger too. It should be noted that increments of the *S*-parameter were smaller with elevating temperature. The growth of the irradiation temperature was followed by the increase in the mobility of interstitial atoms and vacancies. As a result, the probability of both the mutual recombination of point defects and their absorption on sinks was enhanced. The configuration of accumulated defects also changed with growing temperature. The drop of the *R*-parameter values indicated it. For example, in the case of the Fe–Ni alloy [17] exposed to a fluence of 5×10^{22} m^{-2} $R = 2.80 \pm 0.18$ at $T_{irr} = 270$ K and $R = 2.37 \pm 0.13$ at $T_{irr} = 573$ K. The decrease in the *R*-parameter values connected with the predominant formation of two-dimensional clusters as the irradiation temperature was elevated.

At the irradiation temperature of 573 K the situation with the accumulation of defects in the Fe–Ni and Fe–Ni–Ti alloys was different. The growth of the *S*-parameter in the Fe–Ni–Ti alloy was almost fully suppressed as compared to its growth in Fe–Ni (Fig. 1). The Fe–Ni–Ti alloy represented a supersaturated solid solution relative to titanium and underwent the radiation-induced decomposition at this irradiation temperature, which was accompanied by the formation of fine (~5 nm) particles of the Ni_3Ti intermetallic [18]. It was shown [19] that coherent intermetallic particles retarded the accumulation of vacancy defects in austenitic alloys at the elevated irradiation temperatures.

Thus, over the interval of irradiation temperatures studied titanium influenced the accumulation of vacancy-type defects in the Fe–Ni model alloys. Mechanisms of the influence will be discussed below.

Fig. 2 presents the *S*-parameter as a function of the isochronal annealing temperature in the Fe–Ni and Fe–Ni–Ti alloys irradiated up to a fluence of 5×10^{22} m^{-2} at 270, 423 and 573 K. The behavior of the *S*-parameter during annealing of Fe–Ni was considered in detail elsewhere [17]. Therefore, we shall focus on annealing of defects in the Fe–Ni–Ti alloy. The *S*-parameter of this alloy (T_{irr} = 270 K) remained constant up to 450 K, then dropped abruptly, and finally regained its initial value at 650 K. The *S*-parameter also dropped sharply during annealing of Fe–Ni–Ti, which was irradiated at 423 K. The Fe–Ni–Ti sample, which was irradiated at 573 K, was not annealed because of small increments of the *S*-parameter under irradiation (Fig. 1).

Main features of annealing of vacancy-type defects in the titanium-doped alloy are: (1) Annealing of VCs in this alloy started 30 K later than in Fe–Ni. (2) A sharp decrease in the *S*-parameter suggested the dominance of dissociation of vacancy clusters and subsequent absorption of vacancies by sinks. In the Fe–Ni alloy the recovery of the *S*-parameter was delayed at annealing temperatures above 600 K. This observation pointed to the transformation of three-dimensional VCs to thermally more stable two-dimensional clusters representing nuclei of vacancy loops [17]. This was proved most convincingly by annealing of the Fe–Ni sample, which was irradiated at 573 K.

3.1.2. Steels

Fluence dependences of the *S*-parameter for the SS and SS-Ti steels irradiated at 300 and 573 K respectively

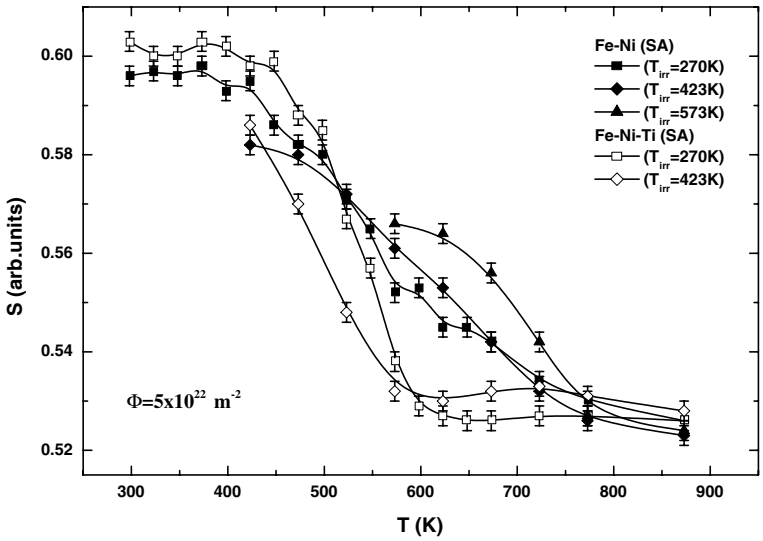

Fig. 2. Evolution of the S-parameter as function of the isochronal annealing temperature in 5×10^{22} m^{-2} electron-irradiated Fe–Ni(SA) and Fe–Ni–Ti(SA) at 270, 423, 573 K, respectively.

are shown in Fig. 3. The initial values of the S-parameter mutually coincided and approached those of the Fe–Ni alloys. At the irradiation temperature of 300 K the S-parameter was much larger than S_v similarly to the situation observed in the Fe–Ni and Fe–Ni–Ti alloys. That is, vacancies in the steels were mobile near room temperature and formed small three-dimensional clusters during their migration. Notice that vacancies were also mobile at these temperatures in the pure Fe–Cr–Ni austenitic alloy [20] having a similar chemical composition. It may be inferred therefore that the presence of molybdenum and other small additions, e.g. interstitial impurities, in the steels had little effect on migration properties of vacancies. This situation is characteristic of other stainless steels as well. For the AISI 316 L steel (its composition is similar to the SS steel composition) it was shown [21] that migration of vacancies began at temperatures, which were even a little lower than in the case of pure Fe–Cr–Ni.

The $S(\phi)$ dependences for the SS and SS-Ti steels were similar at $T_{irr} = 300$ K, i.e. the effect of titanium was not so clearly pronounced as in the Fe–Ni–Ti alloy. At the elevated irradiation temperature the growth of the S-parameter of the titanium-doped steel was consid-

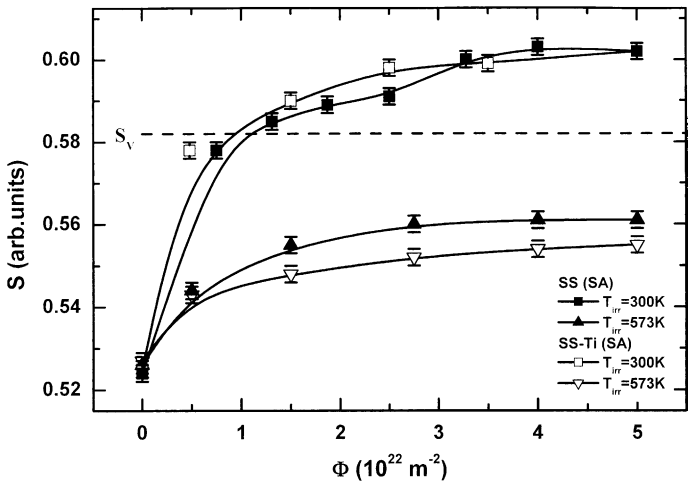

Fig. 3. Variation of the S-parameter as a function of the electron fluence for SS and SS-Ti steels irradiated at 300 and 573 K, respectively. The initial SA state of the samples is the same as in Fig. 1.

erably suppressed. Probably, the radiation-induced formation of intermetallic particles was realized similarly to Fe–Ni–Ti. However, in distinction to pure alloys, precipitation of carbide particles in the steels should be taken into account. The examination by scanning tunneling microscopy (STM) revealed precipitates 7–13 nm in size in samples of the two steels exposed to a fluence of 5×10^{22} m^{-2} at 573 K. The density of these particles in the SS-Ti steel was 2–3 times larger [22]. Unfortunately, the composition and the structure of the precipitates in the steels could not be identified from the STM data.

Dependences of the *S*-parameter on the isochronal annealing temperature of the steels exposed to a fluence of 5×10^{22} m^{-2} at 300 and 573 K are given in Fig. 4. The $S(T_{ann})$ dependence for the SS-Ti steel cold-worked (CW) to 40% is shown for comparison. It is seen that the $S(T_{ann})$ dependences for the irradiated and deformed SS-Ti steel samples are similar, i.e. a similar structure of vacancy clusters was produced in both cases. Notice that VCs in deformed metals represent dominating traps for positrons [23]. The *S*-parameter of SS-Ti started decreasing intensively at annealing temperatures of 500–530 K. Analogously to the Fe–Ni model alloy, annealing of vacancy clusters in the SS steel began 30–50 K lower than in the SS-Ti steel. Thus, titanium atoms stabilized vacancy clusters in the steels too, although this effect was pronounced less than in the alloys. Radiation defects were annealed completely by 700 K. The *S*-parameter of the SS-Ti (CW) steel flattened out at ~600 K because positrons were captured predominantly by dislocations. Annealing of the dislocation structure in the steels will be considered in Section 3.2.

When samples with and without Ti were annealed after irradiation at 573 K, the *S*-parameter decreased continuously to the same extent, i.e. both steels had the same structure of accumulated defects.

3.2. Accumulation and annealing of defects in alloys and steels with a developed initial dislocation structure

3.2.1. Alloys

This section deals with the influence of a developed dislocation structure on the accumulation and annealing of radiation defects. Samples of the Fe–Ni and Fe–Ni–Ti alloys were treated to a solid solution and then were deformed to 40%. To anneal vacancy-type defects, which represent dominating traps for positrons ([23] and Fig. 4), the cold-worked samples were thermally treated at 650 K for 1 h. It was shown [24] that at 650 K vacancy defects were annealed completely and a banded subgrain structure, which was formed during deformation, remained almost unchanged. Dislocations in subgrains formed cellular-network configurations. The average dislocation density of was about 10^{15} m^{-2}. The subgrains, which were extended lengthwise, were 50–400 nm wide. After CW and annealing the Fe–Ni–Ti alloy contained fine intermetallic (Ni_3Ti) particles on dislocations.

Fig. 5 presents fluence dependences of the *S*-parameter of alloys, which were first cold worked and annealed at 650 K for 1 h (the initial DIS state). The irradiation temperature was 300 K. The initial (before irradiation) *S*-parameter of the Fe–Ni alloy approached S_d, which was determined in [24], and was much smaller than S_d in Fe–Ni–Ti. However, dislocation densities determined by TEM were equal in both alloys. It was shown [24] that precipitates partially blocked the capture of positrons by dislocations in Fe–Ni–Ti. This was due to the character of interaction between positrons and

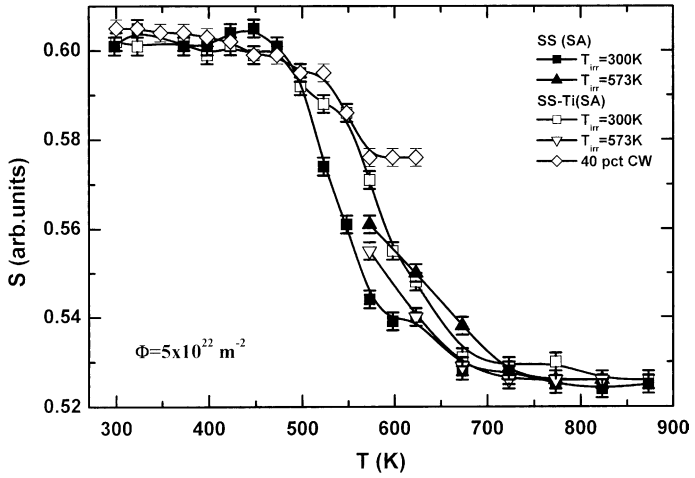

Fig. 4. The *S*-parameter as function of the isochronal annealing temperature in 5×10^{22} m^{-2} electron-irradiated SS(SA) and SS-Ti(SA) at 300 and 573 K, respectively. Also present variation of *S*-parameter with annealing temperature for SS-Ti steel cold worked to 40 pct.

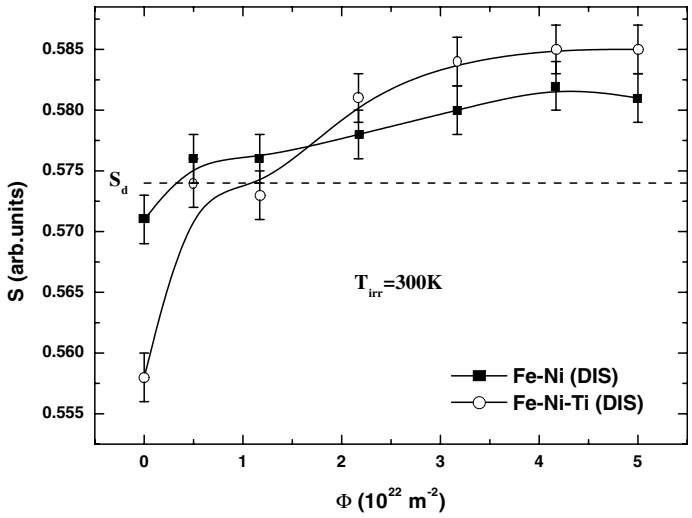

Fig. 5. *S*-parameter variation versus irradiation fluence at 300 K Fe–Ni and Fe–Ni–Ti austenitic alloys. The initial DIS state of the samples (see the text).

dislocations. According to modern representations, dislocation lines themselves represent relatively shallow traps for positrons with the binding energy not larger than 0.1 eV (see [25] and references therein). Thus, it is generally accepted that positrons captured in a shallow trap of a dislocation diffuse rapidly along the line and are eventually trapped and annihilate in point defects associated with the dislocation [11]. For this reason the *S*-parameter of trapped positrons in dislocations (S_d) is just slightly smaller than that of positrons trapped in single vacancies (S_v) (see Figs. 1 and 5). Dislocation lines act as precursor states for transitions into deeper traps. Precipitate particles impede diffusion of positrons along dislocation lines and their capture in deep traps. As a result, trapping becomes less efficient, i.e. the dislocation density, which is sensitive to positrons, diminishes.

When the Fe–Ni alloy was irradiated, the *S*-parameter increased a little and exceeded S_d. Some vacancies were not absorbed by dislocations and formed vacancy clusters. The capture of positrons by these vacancy clusters led to the increase in the *S*-parameter. The value of the *R*-parameter was slightly smaller (2.52 ± 0.13) than in the SA state and represented the weighted average value between R_{cl} and $R_d = 2.17 \pm 0.11$. Correspondingly, it reflected the capture of positrons in two types of traps, namely VCs and dislocations.

The effect of titanium shows itself too. Values of the *S*-parameter were a larger in Fe–Ni–Ti alloy exposed to the fluence above 2×10^{22} m^{-2} (Fig. 5).

The effect of titanium was most evident after annealing of the irradiated samples. Fig. 6 presents $S(T_{ann})$ dependences for alloys having a developed initial dislocation structure, which were irradiated to a fluence of 5×10^{22} m^{-2} at 300 K. The *S*-parameter in Fe–Ni dropped quickly and was constant and approached S_d when the sample was annealed at temperatures above 350 K. In the titanium-doped alloy the *S*-parameter decreased abruptly near 500 K similarly to the situation with Fe–Ni–Ti in the initial SA state (see Fig. 2). The *S*-parameter of the Fe–Ni–Ti alloy regained its initial value at 600 K (Fig. 6).

3.2.2. Steels

The SS and SS-Ti steels, which were cold-worked to 25%, had a cellular-network dislocation structure. Regions, in which dislocations were distributed almost homogeneously and formed irregular networks and tangles, were present. The structure had regions with a weakly pronounced cellular structure. Long unidirectional deformation twins were seen against the cellular-network structure. Stacking faults occurred in both steels. The size of cells in the steels was 200–500 nm and the dislocation density was $\sim 10^{15}$ m^{-2}.

The average dislocation density and the size of the cells changed no considerably when vacancy-type defects were annealed at 573 K (1 h).

Fig. 7 presents the $S(\phi)$ dependence at $T_{irr} = 300$ K for steels after CW and annealing at 573 K for 1 h (the DIS state). Values of the *S*-parameter of the two steels in the DIS state (before irradiation) coincided with S_d values, i.e. positrons were annihilated from dislocation-captured states. Oppositely to the Fe–Ni–Ti alloy, stainless steels are still phase-stable at ~600 K [7] and, therefore, blocking of the capture of positrons by dislocations was not observed. The *S*-parameter increased with the fluence and reached larger values than the *S*-parameter of the alloys (Fig. 5). This phenomenon was especially characteristic of the SS-Ti steel. Thus,

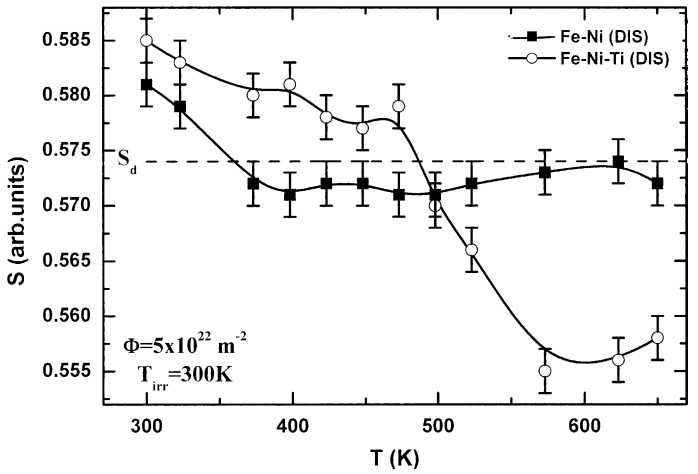

Fig. 6. Evolution of the *S*-parameter as function of the isochronal annealing temperature in 5×10^{22} m^{-2} electron-irradiated Fe–Ni(DIS) and Fe–Ni–Ti(DIS) at 300 K.

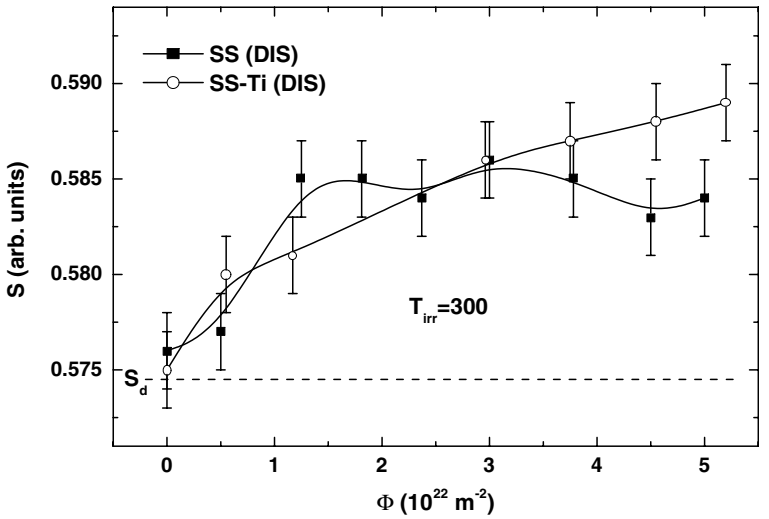

Fig. 7. *S*-parameter variation versus irradiation fluence at 300 K SS and SS-Ti steels. The initial DIS state of the samples (see the text).

the accumulation of vacancy clusters was detected reliably against the background of a large dislocation density, because positrons were captured more efficiently by three-dimensional clusters than by dislocations and single vacancies.

Dependences of the *S*-parameter on the isochronal annealing temperature for steels irradiated with a fluence of up to 5×10^{22} m^{-2} at 300 K are shown in Fig. 8. Annealing of VCs in both steels began at temperatures above 400 K, i.e. 80–100 K lower than in the steels in the initial SA state.

The *S*-parameter approached S_d at 500–600 K, i.e. dislocations were the dominating trapping centers for positrons. Annealing of the dislocation structure in steels represented a more complicated process than, for example, in pure Ni or the single-phase Fe–Ni alloy [24]. The point is that the temperature interval of the cell formation and recrystallization in steels coincides with the interval of formation and growth of carbide and intermetallic precipitates. In this case, a high dislocation density facilitates aging processes [7]. The drop of the *S*-parameter at 600–750 K was due probably to the nucleation of precipitates on dislocations and, hence, blocking of the positron capture (analogously to the Fe–Ni–Ti alloy, see [24] and Section 3.2.1) rather than to annealing of dislocations. The TEM analysis showed that the dislocation density decreased little in CW reactor stainless steels even if they were annealed at 873–923

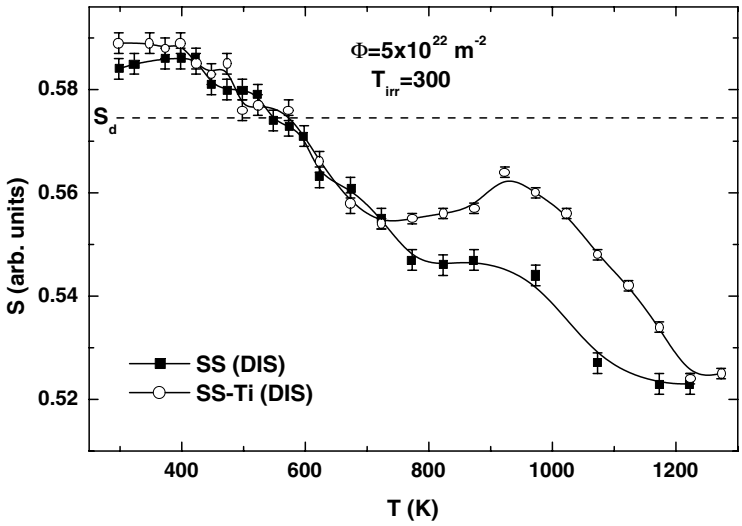

Fig. 8. Evolution of the *S*-parameter as function of the isochronal annealing temperature in 5×10^{22} m^{-2} electron-irradiated SS(DIS) and SS-Ti(DIS) steels at 300 K.

K [12,14]. The *S*-parameter flattened out for both steels above 700–750 K, but the plateau was much higher for the SS-Ti steel. Further, the *S*-parameter of the SS-Ti steel increased at annealing temperatures above 800 K. However, the *S*-parameter of the SS steel did not grow. It dropped above 980 K and regained its initial value at ~1100 K. This was in agreement with a low dislocation density (TEM data) in the steel type 316 at the given temperature [12].

One more distinctive feature of the SS-Ti steel was that the recovery of the *S*-parameter to its initial value was delayed for 180–200 K as compared with the SS-steel. Different behaviors of the *S*-parameter during annealing at 700–1300 K were due to the formation of different types of precipitates in the SS and SS-Ti steels. These phenomena will be considered in more detail below.

4. Discussion

4.1. Effect of titanium

The study demonstrated that addition of Ti as a oversized impurity to the Fe–Ni model alloys and Fe–Cr–Ni steels had a considerable effect on the accumulation and thermal stability of vacancy defects. These defects represented small three-dimensional VCs (at the irradiation temperature of ~300 K). It is known [23] that impurities, which interact with vacancies, represent nucleation centers of vacancy clusters. When the concentration of the nuclei is high (suitable impurities), VCs are larger in number and smaller in size. Ti atoms forming nuclei of vacancy clusters trapped migrating vacancies. As a result, absorption of vacancies by sinks became less probable and fine VCs had an enhanced concentration, leading to a stronger increase in the *S*-parameter of the Fe–Ni–Ti alloy under irradiation at 270 K and 423 K.

Thus, it may be inferred that at irradiation temperatures of 270–423 K the Ti-doped alloy and steel (the initial SA state) formed an enhanced concentration of fine titanium-decorated VCs, which were thermally stable up to 450 K.

Let us see how this inference correlates with the HVEM data for the Ti-doped Fe–Cr–Ni alloy. Watanabe et al. [1] showed that addition of titanium delays the formation of clusters of vacancy-type defects (loops and stacking fault tetrahedra) up to 450 K. At first sight, this finding contradicts our results. However, there is no contradiction. Small Ti-stabilized VCs are not seen in an electron microscope. At temperatures above 450 K, when the interaction between Ti atoms and VCs weakens, large clusters, which are observable by HVEM, are formed under irradiation up to doses of 0.1 dpa.

The effect of titanium shows itself at the elevated irradiation temperature (573 K) too, but its mechanism is different. The Fe–Ni–Ti alloy and the SS-Ti steel represent supersaturated solid solutions relative to titanium. As was mentioned in Section 3.1, the radiation-induced decomposition and the formation of fine intermetallic particles were observed in Fe–Ni–Ti and particles of intermetallics and, probably, carbides appeared in SS-Ti. It has long been known [5] that intermetallic particles decrease vacancy supersaturation. Possible mechanisms of this phenomenon were discussed in [19].

4.2. Role of the dislocation structure

It was shown in Section 3.2 that the accumulation of VCs under irradiation at room temperature was reliably detected against the background of a high average dislocation density. The effect of Ti atoms in the solid solution shows itself too. It is especially illustrative if one considers annealing of VCs in the model alloys in the initial DIS state (Fig. 6). An ensemble of VCs having different multiplicities was formed under irradiation. Clusters with a smaller multiplicity were less stable and dissociated earlier. Released vacancies either vanished on sinks or were absorbed by larger clusters. The distance between dislocations (sinks) in the deformed alloy was 2 orders of magnitude smaller than in the initial SA state. Therefore, the dominating process was vanishing of vacancies on dislocations. This conclusion was confirmed by a sharp decrease in the *S*-parameter of the Fe–Ni alloy at lower annealing temperatures as compared with the SA state (see Fig. 2).

Thermal stability of clusters decorated with titanium atoms depended on the efficiency of the vacancy-titanium interaction (the binding energy). Therefore, the effect of a high dislocation density was less in this case. Indeed, the *S*-parameter of Fe–Ni–Ti (DIS) decreased sharply at the same temperature (~500 K) as in the SA state.

The model of the positron capture on two centers [27] was used to estimate the cluster concentration C_{cl} in samples of the SS steel and the Fe–Ni alloy in the initial SA and DIS states exposed to a fluence of 5×10^{22} m^{-2} at ~300 K. According to the estimates, C_{cl} decreased one and a half (SS) or twice (Fe–Ni) in the DIS samples as compared to the samples in the initial SA state. The decrease in the concentration of VCs by times and not by orders of magnitude might be related to an inhomogeneous distribution of dislocations in the deformed samples. Despite a high average dislocation density, it was orders of magnitude lower in the cells than in the walls and, therefore, radiation defects in the cells were accumulated by a scheme typical of the SA state. Also, if one considers that the migration energy of vacancies in the steel was ≈0.9 eV [13], their diffusion length at 300 K was equal to units of nm, which was much smaller than the cell size.

4.3. Annealing of dislocations in steels: effect of nucleation of precipitates in steels on the interaction between positrons and dislocations

It was mentioned in Section 1 that studies of annealing of CW stainless steels revealed a low sensitivity of positrons to dislocations [12,13]. An analogous situation was observed in our case too. The *S*-parameter of the DIS steels began decreasing when the samples were annealed at a temperature above 600 K, at which dislocations were immobile (Fig. 8). This fact was also observed in our study into annealing of a cold-deformed Fe–Ni–Ti model alloy (see [24] and Section 3.2.1). It was shown that nuclei of the γ'-phase, which were formed on dislocations during annealing, blocked the capture of positrons on dislocations. Positron trapping was blocked not only by nuclei of the ordered phase, but also by Cottrell's atmospheres of excess atoms (for example, C, Ti and Cr). Indeed, the suppression of the capture of positrons by dislocations was discovered in dilute Al–Cu and Al–Mg alloys [26] when Cu and Mg atoms segregated on dislocation lines without formation of phases. The SS and SS-Ti steels represented supersaturated solid solutions and, therefore, the formation and the growth of segregates on dislocations led to appearance of precipitate particles. These particles were able not only to block the capture of positrons by dislocations and pin the dislocations, but also could serve as positron trapping centers themselves. Precipitates could capture positrons either as a result of preferred affinity [28,29] or owing to the incoherence of particles by misfit dislocations [30]. According to calculations [29], most of carbides have not a preferred affinity as compared with host materials. Therefore, positrons can be captured only by misfit dislocations, which are connected with carbide particles.

Considerably different behaviors of the *S*-parameter in the SS and SS-Ti steels annealed above 700 K were explained by the formation of different types of particles.

The TEM examination of the SS steel (the initial SA state), which was aged at 923 K for 20 h, revealed the presence of fine (5–7 nm) $M_{23}C_6$ particles, which were concentrated predominantly on grain boundaries. We did not detect the capture of positrons by $M_{23}C_6$ particles in the SS steel either after aging of the SA state or during annealing of the DIS state. From Fig. 8 it is seen that the *S*-parameter remained constant at annealing temperatures of 750 to 1000 K. This fact was explained probably by a low carbon concentration (0.03%) of the SS steel and, hence, the density of $M_{23}C_6$ particles was smaller than the sensitivity limit of PAS or positrons had a low sensitivity to these particles because of a slight mismatch (~1.3% [31]).

The tendency to the growth of the *S*-parameter during annealing of the SS-Ti steel (the initial DIS state) at a temperature above 700 K was related to the dominating formation of titanium-containing precipitates. Indeed, the TEM examination of the SS-Ti steel (the initial SA state), which was aged under conditions similar to those used for the SS steel (973 K, 20 h), revealed the presence of fine particles both on grain boundaries and dislocations. The fine particles were identified as TiC carbides. A comprehensive TEM analysis of foils revealed a ripple-type contrast in extinction contours. It may be asserted therefore that particles presumably of the Ni_3Ti γ'-phase precipitated along with fine TiC

carbides during aging. However, similarly to the aged SS steel, the *S*-parameter of the aged SS-Ti steel did not differ from the *S*-parameter in the SA state. The capture of positrons by coherent Ni_3Ti particles did not reveal in an aged Fe–Ni–Ti model alloy [24]. Those particles were mismatched in the austenitic matrix by less than 1% [5]. As far as TiC particles are concerned, after aging they were detected mainly on dislocations, whose density was small ($\sim 10^{11}$ m^{-2}) in the SA state. It may be assumed therefore that the density of TiC particles was lower than the PAS sensitivity limit.

On the other hand, at the annealing temperature of 923 K the deformed SS-Ti steel had a maximum value of the *S*-parameter (above 700 K), which could be related to the capture of positrons by TiC precipitates. Indeed, in the TEM studies reported earlier [14] the formation of TiC precipitates in a cold-worked titanium-modified stainless steel was observed over the temperature interval of 923 to 1073 K. Those studies demonstrated also that dislocations controlled precipitation of fine TiC particles. The TiC precipitates had a face-centered cubic lattice with an extremely large mismatch in the austenitic matrix and the lattice parameters differing by 19–21%. A large strain arising from this lattice mismatch led to generation of misfit dislocations on the TiC-matrix interface [32]. As was shown in [33], these misfit dislocations represent effective traps for positrons. The variation of the *S*-parameter of the SS-Ti steel at temperatures from 823 to 1073 K corresponded to the capture of positrons on the interface between a TiC precipitate and the matrix. The growth of the *S*-parameter was due to the increase in the density of TiC particles, whereas the decrease in the *S*-parameters at temperatures above 1000 K was related to the coarsening of the particles during recrystallization [14]. The kinetics of formation and growth of TiC particles in a Ti-modified stainless steel were studied more comprehensively by PAS in [32].

The obtained results show that the response of positrons to processes, which take place during annealing of dislocations in stainless steels, strongly depends on the type and density of precipitates, i.e. the type and the concentration of alloying additions. For example, the carbon concentration (0.05 wt%) of the D-9 steel (its composition is similar to the SS-Ti steel composition [33]) is higher than the carbon concentration of the SS-Ti steel and, correspondingly, the TiC effect is more pronounced [32]. On the other hand, blocking of the capture of positrons by dislocations is determined by the efficiency of segregation of alloying atoms on dislocations at relatively low annealing temperatures.

It should be noted finally that the sensitivity of positrons to the formation of segregates and, subsequently, phase particles on dislocations could be used in practical studies of deformed nuclear materials.

5. Conclusions

Positron annihilation spectroscopy was used to ascertain how titanium and cold working influenced the accumulation and annealing of defects in Ti-modified fcc Fe–Ni alloys and Fe–Cr–Ni stainless steels exposed to electron irradiation. The main results reduce to the following:

1. It was found that vacancies interacted with titanium atoms. As a result, at the irradiation temperatures of 270–423 K the Ti-doped alloy and steel (the initial SA state) formed an enhanced concentration of fine vacancy clusters decorated with titanium, which were thermally stable up to 450 K.
2. When the irradiation temperature was increased (573 K), vacancy defects accumulated less in the Ti-modified alloys and steels because of the radiation-induced formation of Ni_3Ti intermetallic particles.
3. It was shown that a high initial dislocation density in the steel and alloy samples caused a several-fold decrease in the accumulation of vacancy clusters as compared to the samples in the initial SA state. A local inhomogeneity of the dislocation structure influenced the evolution of radiation damageability, specifically, the accumulation of vacancy defects in cells analogously to the solid solution.
4. A high-temperature stage (850–1070 K) was detected during annealing of a titanium-doped deformed steel. This stage was related to the formation of fine particles of TiC carbides during movement of dislocations.

Acknowledgement

The authors wish to thank Dr N.L. Pecherkina for her assistance in characterization of the microstructure of the initial solution-annealed, aged and deformed samples. This work was supported by Russian Foundation for Basic Research (project no. 04-02-16053) and the Program of Support for Leading Scientific Schools (project no. NSh-639.2003.2).

References

[1] H. Watanabe, T. Muroga, N. Yoshida, J. Nucl. Mater. 239 (1996) 95.
[2] W. Kesternich, D. Meertens, Acta Metall. 34 (1986) 1071.
[3] R.M. Bothy, T.M. Williams, J. Nucl. Mater. 152 (1988) 123.
[4] W. Kesternich, J. Nucl. Mater. 127 (1985) 153.
[5] V.V. Sagaradze, V.M. Nalesnik, S.S. Lapin, V.M. Alyabiev, J. Nucl. Mater. 202 (1993) 137.

[6] W.G. Wolfer, B.B. Glasgow, Acta Metall. 33 (1985) 1997.
[7] B. Weiss, R. Stickler, Metall. Trans. 3 (1972) 851.
[8] P. Hautojarvi (Ed.), Positrons in Solids, Springer, Berlin, 1979.
[9] A. Dupasquier, A.P. Mills (Eds.), Positron Spectroscopy of Solids, North-Holland, Amsterdam, 1994.
[10] M. Eldrup, B.N. Singh, J. Nucl. Mater. 251 (1997) 132.
[11] T. Wider, S. Hansen, U. Holzwarth, K. Maier, Phys. Rev. B 57 (1998) 5126.
[12] W.B. Gauster, W.R. Wampler, W.B. Jones, J.A. van den Avyle, in: R.R. Hasiguti, K. Fujiwara (Eds.), Proceedings of the 5th International Conference on Positron Annihilation, Japan Inst. of Metals, Sendai, 1979, p. 125.
[13] U. Holzwarth, A. Barbieri, S. Hansen-Ilzhofer, P. Schaaff, M. Haaks, Appl. Phys. A 73 (2001) 467.
[14] W. Kesternich, Phil. Mag. A 52 (1985) 533.
[15] J. Morillo, C.H. de Novion, J. Dural, Radiat. Eff. 55 (1981) 67.
[16] V.L. Arbuzov, S.E. Danilov, A.P. Druzhkov, Phys. Status Solidi A 162 (1997) 567.
[17] V.L. Arbuzov, A.P. Druzhkov, S.E. Danilov, J. Nucl. Mater. 295 (2001) 273.
[18] K.V. Shalnov, V.L. Arbuzov, S.E. Danilov, A.P. Druzhkov, Proceedings of the 1st International Congress on Radiation Physics, High Current Electronics, and Modification Materials, vol. 1, Tomsk, Russia, 2000, p. 145.
[19] A.P. Druzhkov, V.L. Arbuzov, D.A. Perminov, K.V. Shalnov, Fiz. Met. Metalloved. 96 (2003) 74;
A.P. Druzhkov, V.L. Arbuzov, D.A. Perminov, K.V. Shalnov, Russ. Phys. Met. Metallogr. 96 (2003) 509, English Translation.
[20] D. Huguenin, P. Moser, F. Vanoni, J. Nucl. Mater. 169 (1989) 73.
[21] P. Erhardt, in: Landolt-Bornstein, Numerical Data and Functional Relationships in Science and Technology, Group III: Crystal and Solid State Physics, in: H. Mehrer (Ed.), Atomic Defects in Metals, vol. 25, Springer-Verlag, Berlin, Heidelberg, 1990, p. 88.
[22] A.P. Druzhkov, V.L. Arbuzov, S.E. Danilov, K.V. Shalnov, V.V. Sagaradze, Proc. 6th Russian Conference on Reactor Materials Science, vol. 3, Dimitrovgrad, Russia, 2000, p. 125, Part 1.
[23] G. Dlubek, R. Krause, O. Brummer, Z. Michno, T. Gorecki, J. Phys. F: Met. Phys. 17 (1987) 1333.
[24] V.L. Arbuzov, A.P. Druzhkov, N.L. Pecherkina, S.E. Danilov, D.A. Perminov, V.V. Sagaradze, Fiz. Met. Metalloved. 92 (2001) 75;
V.L. Arbuzov, A.P. Druzhkov, N.L. Pecherkina, S.E. Danilov, D.A. Perminov, V.V. Sagaradze, Rus. Phys. Met. Metallogr. 92 (2001) 70, English Translation.
[25] U. Holzwarth, P. Schaaff, Phys. Rev. B 69 (2004) 094110.
[26] E. Hashimoto, M. Iwami, Y. Ueda, J. Phys.: Condens. Matter. 6 (1994) 1611.
[27] A.P. Druzhkov, V.L. Arbuzov, D.A. Perminov, Fiz. Met. Metalloved. 94 (2002) 75;
A.P. Druzhkov, V.L. Arbuzov, D.A. Perminov, Rus. Phys. Met. Metallogr. 94 (2002) 68, English Translation.
[28] M.J. Puska, P. Lanki, R.M. Nieminen, J. Phys.: Condens. Matter 1 (1989) 6081.
[29] G. Brauer, M.J. Puska, M. Sob, T. Korhonen, Nucl. Eng. Des. 158 (1995) 149.
[30] R. Krause, G. Dlubek, O. Brummer, Proceeding of the European Meeting on Positron Studies of Defects, vol. 1, Part 1, PL-7, Wernigerode, 1987.
[31] J. Dryzek, C. Wesseling, E. Dryzek, B. Cleff, Mater. Lett. 21 (1994) 209.
[32] P. Gopalan, R. Rajaraman, B. Viswanathan, K.P. Gopinathan, S. Venkadesan, J. Nucl. Mater. 256 (1998) 229.
[33] R. Rajaraman, P. Gopalan, B. Viswanathan, S. Venkadesan, J. Nucl. Mater. 217 (1994) 325.